Challenge in the speciation of nitrogen-containing compounds in heavy petroleum fractions by high temperature comprehensive two-dimensional gas chromatography

Thomas Dutriez[a], Julie Borras[a], Marion Courtiade[a,*], Didier Thiébaut[b], Hugues Dulot[a], Fabrice Bertoncini[a], Marie-Claire Hennion[b]

[a] IFP Energies nouvelles, Rond-point de l'échangeur de Solaize, BP 3, 69360 Solaize, France
[b] ESPCI, PECSA UMR CNRS 7195, LSABM, 10 rue Vauquelin, 75231 Paris Cedex 05, France

ARTICLE INFO

ABSTRACT

Extending the knowledge related to nitrogen-containing compounds presents an important interest for the petroleum industry due to their implication in atmosphere pollution as well as their inhibitive or refractive behaviour towards hydroprocessing. Most of the nitrogenated species are concentrated in heavy petroleum cuts. As no analytical method is resolutive enough for these heavy cuts, particularly regarding nitrogen-containing compounds, a new approach is needed. For this reason, this study focuses on the development of a GC × GC technique, through the hyphenation of a specific NCD detector with a GC × GC system at high temperature. The performances of highly polar thermally stable stationary phases, in particular those composed of promising ionic liquids, were monitored in normal and reversed configurations. Subsequently, after the extraction of neutral or basic compounds by adsorption on an ion-exchange resin, a first quantitative determination was attempted for a straight-run and a direct coal liquefaction vacuum gas oils. This study led to a better understanding of the behaviour of highly aromatic N-compounds by 2D-GC including an ionic liquid phase as well as a deeper N-characterization of heavy petroleum fractions.

© 2010 Published by Elsevier B.V.

1. Introduction

Despite the relatively low proportion of nitrogen element in crude oils, nitrogen-containing compounds are of great interest for petroleum industry. As a matter of fact, N-compounds affect the formation of fouling and gum, but also promote the corrosion in fuels [1]. Their presence in fuel oils or Fluid Catalytic Cracking feeds is also continuously reduced in order to avoid the release of nitrogen oxides (NOx) in the atmosphere after their combustion. As the quality of worldwide reserves constantly decrease, the interest for heavy cuts is incessantly growing. This implies the need to deal with higher nitrogen contents. Usually, nitrogenated species are removed from heavy petroleum cuts, such as vacuum gas oils (VGOs) (350–600 °C), during hydrotreatment processes via hydrodenitrogenation reactions. This essential purification step is generally performed before the conversion processes (hydrocracking or catalytic cracking) to prevent catalysts from being poisoned.

Organic nitrogen compounds can be differentiated depending on their chemical structures: the ones with a basic behaviour are
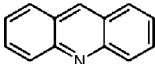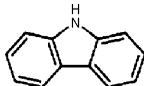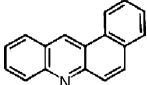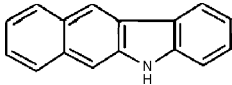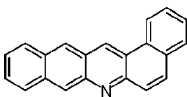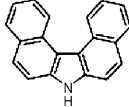
based on a pyridine core; the ones with a neutral behaviour are based on a pyrrole core. Nitrogen-containing compounds in heavy petroleum cuts (350+ °C) are usually composed by highly alkylated polyaromatic structures, such as carbazoles, benzocarbazoles, dibenzocarbazoles (neutrals) and acridines, benzoacridines or dibenzacridines (basics) (Table 1) [2].

Nitrogenated species have negative implications on the refining of heavy cuts [3]. Neutral N-compounds are actually considered as refractories to hydroconversion reactions. On the other hand, basic ones show an inhibitive behaviour towards the hydrotreatment step [4,5], especially hydrodesulfurization reactions. Moreover they poison the acidic catalysts sites [3] during hydroconversion processes. In addition, the presence of basic nitrogen-containing compounds increases the catalyst deactivation by coking. Therefore, in order to better understand the reactions implemented during hydroprocessing, a detailed characterization of nitrogenated species in heavy petroleum cuts is necessary. Consequently, improvements in the design of more efficient catalysts could be envisaged.

Several analytical methods are dedicated to the speciation of nitrogenated species in petroleum products, for instance: GC hyphenated to AED, NCD or MS [6] but also LC techniques hyphenated to MS [7]. Granted light cuts, such as gasoline, can be fully

* Corresponding author. Tel.: +33 04 37 70 20 76; fax: +33 04 37 70 27 45.
E-mail address: marion.courtiade@energiesnouvellesifp.fr (M. Courtiade).

Table 1
Typical organic nitrogen-containing structures in heavy petroleum cuts.

Basics		Neutrals	
Acridine		Carbazole	
Benzo(a)acridine		Benzo(b)carbazole	
Dibenzo(a,i)acridine		Dibenzo(c,g)carbazole	

characterized by 1DGC. However, it remains difficult to deal with heavier cuts, in particular for a quantitative purpose.

Concerning middle-distillates, breakthrough advances were done these last years, in particular since the implementation of bidimensional gas chromatographic techniques (GC × GC) [8]. For complex matrices, the use of two separation dimensions interacting with different mechanisms allows to avoid coelutions, thank to a high peaks capacity [9]. Peaks are indeed scattered in 2D contour plots structured by each separation dimension. Consequently, GC × GC has led to innovative results in the characterization of middle-distillates [10,11] by mapping the matrices by carbon atoms number and by chemical families. As far as the speciation of N-compounds is concerned, the hyphenation of nitrogen specific detectors (NPD [12], AED [13], NCD [14]) was successfully implemented with GC × GC. In particular, the use of a NCD detector allowed the setting of a new benchmark [15,16] for the quantitative speciation of middle distillates. Very recently the characterization of nitrogen-containing compounds in heavy gas oils was reported by von Muhlen et al. [17].

Concerning heavy fractions like VGOs, almost no information is available about nitrogenated species [18,19] except for the elemental composition or distributions by boiling point [20]. Although a group type quantification can be obtained by MS methods [21], the fraction containing most of the nitrogenated species (resins fraction) is usually removed beforehand, as it is suspected to distort the results [22]. Recently, the implementation of the Fourier Transform Ion Cyclotron Resonance Mass Spectrometry (FT-ICR/MS) has offered a new way for a full identification of nitrogen compounds in petroleum cuts [23]. Even though the lack of a reliable quantitative procedure has precluded, until now, its use for the integration in processes optimization steps. On the other hand the extension of the molecular range attainable by GC × GC is still challenging [24,25]. However, the tuning of the GC × GC system in borderline application conditions (i.e. very high modulation period and high temperature) allowed to give innovative quantitative data for hydrocarbons contained in VGOs (more than 1 million of compounds) [25]. This analytical approach appears useful for the study of conversion processes [26,27]. The main limitations are the lack of selectivity for polar dimensions at high temperature which can induce high coelutions.

However, the thermal stability of polar stationary phases is continuously enhanced. Some efforts were made for specific treatments of sol–gel phases [28] and new phases based on ionic liquids have recently been proposed [29]. These belong to a class of non-molecular solvents containing a combination of cations and anions [30]. This promising design tends to reach new selectivities due to various solvation interactions. Another advantage of ionic liquid phases is their low vapour pressures, which grant them high thermal stabilities [31]. Consequently, new possibilities have been opened up for the tuning of selectivity in GC × GC [32,33], but also for the developments of GC × GC × GC [34].

Considering all these reasons, the hyphenation of a high temperature comprehensive gas chromatography (HT-2D-GC) with a specific NCD detector was implemented in this study. Most of the available thermal stable stationary phases, including a newly developed ionic liquid, were investigated in normal or reversed configurations. 2D separation criteria, like resolution or asymmetry, were monitored on 2D contour plots of a test mixture of model compounds. Then, the use of an ion-exchange chromatography to separate neutral and basic compounds allowed an easier attribution of 2D elution zones. Subsequently a quantitative analysis of nitrogen-containing compounds in two matrices, in a vacuum gas oils boiling point range, was performed.

2. Experimental details

2.1. Elemental characterization

Total nitrogen and basic nitrogen contents of petroleum samples were determined according to standardized methods. Concerning the determination of the total nitrogen content, the NF M07-058-92 method was applied to samples ranging from 1 to 500 ppm N, using an Antek 9000 analyzer, and to samples between 100 and 1000 ppm N, using a Lumazote Eraly AC 30M analyzer. The total nitrogen content of highly nitrogen concentrated samples (more than 1000 ppm N) was determined using a Thermofinnigan CHN NA2100 analyzer, according to the ASTM D5291-02 method. The basic nitrogen content was determined by potentiometry, according to the ATSM D-4729-03 standard method.

2.2. Ion-exchange chromatography

An ion-exchange chromatography, adapted from the literature [35], was used to separate nitrogen-containing compounds, basic and neutral types, from feed stock samples. This separation was achieved using an ion-exchange resin (Amberlyst A-15), whose acidic sites can specifically retain basic nitrogenated species. Hydrocarbons and neutral N-compounds were first eluted using methanol. Then, basic species were desorbed from the resin using a dichloromethane/ammonium mixture and then a methanol/ammonium mixture. Solvents were purchased from Sigma–Aldrich (St Quentin Fallavier, France). Finally, the LC mobile phase was evaporated from the two fractions and a "Neutral fraction" and a "Basic fraction" were obtained. The other compounds contained in the feedstock sample were recovered in the two fractions. Total and basic nitrogen contents were determined for both fractions in order to evaluate the separation efficiency. Neutral and basic fractions were first diluted in toluene (about 40 ppm of the

Table 2
Composition of test mixtures TM1 and TM2.

Compounds	Concentration (ppm N)	Peaks
TM1		
Neutrals		
Carbazole	5.51	1
3-Ethylcarbazole	5.58	2
Tetrahydrobenzocarbazole	3.84	3
Benzo(b)carbazole	2.79	4
8-Methylbenzo-11H-carbazole	2.62	5
Dibenzo(c,g)carbazole	5.35	6
Basics		
Acridine	5.53	7
Benzo(a)acridine	4.97	8
7,10-Dimethylbenzoacridine	1.56	9
Dibenzo(a,c)acridine	5.01	10
TM2		
Acridines		
Acridine	8.84	7
9-Methylacridine	8.02	11
Benzoacridines		
Benzo(a)acridine	7.96	8
7,10-Dimethylbenzoacridine	6.26	9
Dibenzoacridines		
Dibenzo(a,c)acridine	7.95	10
Dibenzo(c,h)acridine	2.31	12

total nitrogen content) to be analysed in the adapted HT-2D-GC configuration.

2.3. Petroleum samples and test mixtures

In order to set the adapted GC × GC configuration, but also to help the identification of 2D elution zones, three synthetic test mixtures of nitrogen-containing compounds were prepared in toluene (from 1 to 9 ppm N). The composition of these test mixtures (TM1, TM2, TM3) are in Tables 2 and 3. Model N-compounds were purchased from Chiron (Trondheim, Norway), Sigma–Aldrich (St Quentin Fallavier, France) and Alfa Aesar (Schiltigheim, France). Two vacuum gas oils were supplied by IFP Energies Nouvelles Lyon (Table 4). The first one (VGO) comes from a mixture of several straight-run vacuum gas oils. The second one is a coal liquefaction (CL) product coming from a direct hydroliquefaction process.

Table 3
Composition of test mixtures TM3.

Compounds	Concentration (ppm N)	Peaks
TM3		
Carbazoles		
Carbazole	4.83	1
2-Methylcarbazole	1.78	13
9-Methylcarbazole	4.46	14
3-Ethylcarbazole	4.12	2
9-Ethylcarbazole	4.14	15
9-Isopropylcarbazole	3.86	16
Pentamethylcarbazole	5.22	17
9-Octylcarbazole	2.89	18
Tetra-tertbutylcarbazole	4.95	19
1,2,3,4 Tetrahydrocarbazole	4.72	20
Benzocarbazoles		
Benzo(b)carbazole	1.48	4
8-Methylbenzo-11H-carbazole	1.39	5
Ethylmethylbenzocarbazole	1.25	21
Dibenzocarbazoles		
Dibenzo(c,g)carbazole	3.02	6
Dibenzo(a,i)carbazole	1.21	22

2.4. HT-2D-GC experiments

The GC × GC system consists of an in-house modified 6890 chromatograph (Agilent, Massy, France) equipped with a CO_2 dual jet modulator [36]. 2D modulation was carried out at the beginning of the second column (modulation period: 30 s). The injection was carried out by an on-column injector programmed from 90 to 350 °C with a 50 °C/min temperature gradient. The specific nitrogen detection was performed with a NCD (255 Dual Plasma, Sievers, Boulder, USA). Data acquisition frequency was set to 100 Hz and operating conditions recommended by the manufacturers were used for the NCD detection. Helium was used as carrier gas at constant pressure. Different column sets were performed and are in Table 5. Raw data of FID signals were acquired using the Chemstation software (Agilent, Massy, France) and exported as a CSV-file for further data processing. GC × GC contour plotting, retention time measurement, blobs fitting and peaks integration were performed using 2DChrom™ (Thermo, Milano, Italy). Intensities were visualized using contrasted colours, ranging from pale blue to dark blue respectively for minor and major peaks.

3. Results and discussion

3.1. Investigations of several 2D configurations

The analysis by GC or GC × GC of high boiling point compounds requires high temperature conditions. Even if efforts have been made in terms of the thermal stability of stationary phases, the choice of polar columns is still limited. Therefore, a classical BPX-50 was chosen as well as a promising ionic liquid phase (IL-59). Experiments were focused on geometric considerations and also on column combinations: normal and reversed configurations. Thus, five operating conditions were retained (Table 5) keeping in mind the difficult equilibrium between the lowering of elution temperatures and high efficiencies of separation [24]. The test mixture 1 (TM1) was used to monitor the different applied conditions. This mixture was composed of neutral or basic polyaromatic N-species, which are supposed to be present in heavy petroleum fractions.

2D contour plots corresponding to the test mixture TM1 are presented in Fig. 1. For normal and reversed columns combinations, sets A, B and D, E, peak apices were extracted by the 2D software and compiled together to facilitate the visualization of the retention time variations. A very high modulation period (30 s) was selected because our goal was more to achieve the best group type separation rather than to operate a "strict" GC × GC (with at least three samplings by peaks of first dimension).

Concerning normal configurations, set A corresponds to the operating conditions implemented for the hydrocarbons analysis in VGOs [24]. A distinction by aromatic rings number was observed along the second dimension granted to the BPX-50 (developing π–π interactions). In order to prevent the high band broadening of N-compounds in the second dimension, a longer first dimension was implemented (set B). This allows increasing the elution temperature of solutes at the modulation step. As a consequence, the dimension of the secondary column was adapted in order to keep an adequate peaks scattering on the 2D contour plot.

In set C, the ionic liquid phase was implemented in a normal configuration (set C) with the same first column as set B. Due to the very high retention of neutral nitrogen-containing compounds on the IL-59, a very short secondary column was preferred. Even under these conditions, the retention time of dibenzo(c,g)carbazole was longer than the modulation period. Surprisingly, basic N-compounds were almost not retained on the IL-59, while neutral ones were strongly retained. Reasons can be found in the chemical interactions between the stationary

Table 4
Physical characteristics and elementary composition of the two studied VGOs.

Samples	Density at 15 °C (g/cm³)[a]	Total sulphur (% S)[b]	Total nitrogen (ppm N)[c]	Basic nitrogen (ppm N)[d]	Boiling point interval (°C)[e]
VGO	0.9237	2.41	836	235	366–533
Direct CL	1.0434	0.02	6148	3255	342–477

[a] Determined by NF ISO12185.
[b] Determined by NF ISO14596 or ISO20884.
[c] Determined by NF 07058 or ASTM D4629.
[d] Determined by ATSM D-4729-03.
[e] Determined by SimDist (ASTM D-2887) (5–95 wt%).

phase and N-compounds. The main difference between basic and neutral N-compounds is the presence of a N–H bond for neutral ones which can strongly interact through hydrogen bonds (dipole–dipole interactions). Actually, ionic liquid phases are known to produce strong hydrogen bonding interactions [29] (with alcohols or amines), as theses phases have free pairs of electrons on their anions or cations. Moreover, the selection of specific cations can emphasize or minimize this behaviour. The chemical composition of IL-59 is not revealed yet, but it is probably based on a bis(trifluoromethanesulphonyl)imide (NTf_2^-) anion. Furthermore for set C, a selectivity based on π–π interactions is still observed along the second dimension.

Concerning reversed phase configurations (sets D and E), a mid-polar BPX-50 was implemented in the first dimension. Set D was adjusted to almost the same column geometry as set B for a better comparison. Actually, a very high retention of polyaromatic N-compounds was observed on the first column to a point where their elution temperature is so elevated that they can not be correctly separated in the second dimension. To solve this problem, a shorter BPX-50 column and a longer apolar secondary column were selected for set E. Even in this case, N-compounds of the test mixture (TM1) were highly retained on BPX-50, and the second dimension did not provide suitable scatterings. However, a distinction based on aromatic rings number was still performed on 2D contour plots.

3.1.1. Monitoring of 2D separation criteria

In order to validate qualitative remarks between 2D contour plots of each set, 2D separation criteria were applied. Therefore, the system selectivity was estimated by the 2D resolutions (Rs_{2D}) calculation (Fig. 2). Although methods based on valleys to peaks ratio [37] have been recently proposed for non-Gaussian peaks, the 2D resolution introduced by Giddings [8] appears more useful. Thus, Rs_{2D} between solutes A and B is defined as the Euclidian norm of the resolution over the two axes from Eq. (1),

$$Rs_{2D} = \sqrt{{}^1Rs^2 + {}^2Rs^2} \tag{1}$$

where ${}^1Rs$ and ${}^2Rs$ are respectively the resolutions between the two solutes along the first and the second dimension. The 2D resolution can also be given as in Eq. (2),

$$Rs_{2D} = \sqrt{\frac{2(\Delta^1 t_R)^2}{({}^1\omega_A + {}^1\omega_B)^2} + \frac{2(\Delta^2 t_R)^2}{({}^2\omega_A + {}^2\omega_B)^2}} \tag{2}$$

where ${}^1\omega$ and ${}^2\omega$ are the peak widths along each dimension at 10% for compounds A and B. $\Delta^1 t_R$ and $\Delta^2 t_R$ are the difference of retention times between the apices of the two compounds. Peak widths (${}^1\omega$) in the first dimension are considered equal to the product of the number of modulations. Thereby, the 2D resolutions according to the acido-basic type of N-compounds were monitored (Fig. 2A), between acridine and carbazole, or benzo(a)acridine and benzo(b)carbazole. Previous qualitative remarks were confirmed as set C, with the ionic liquid phase, achieves the best separation on the basis of acido-basic properties. Besides, intraclass 2D resolutions (by alkylation) (Fig. 2B) were determined for several group types (carbazole/3-ethylcarbazole, benzo(b)carbazole/8-methylbenzo-11H-carbazole and benzo(a)acridine/7,10-dimethylbenzoacridine). Sets B, C and D provided the best results for a separation by carbon atoms number. Then, interclass 2D resolutions (by π–π interactions, i.e. aromatic group types) were estimated for each set (Fig. 2C) for carbazole/benzo(b)carbazole, benzo(b)carbazole/dibenzo(c,g)carbazole, acridine/benzo(a)acridine and benz(a)acridine/dibenzo(a,i)acridine, but also for the naphtheno-aromatic distinction (tetrahydrobenzocarbazole/benzo(b)carbazole). Regarding the group type separation, sets B, C and D gave the best results.

As the peak shape of heavy hydrocarbons [38] can be altered during the GC × GC process, especially during the cryogenic modulation step, a resulting asymmetrical 2D peak can be observed. Recently, 2D asymmetry (As_{2D}) [24] was introduced, in order to quantify the observed peak asymmetry in both dimensions. This idea is based on an empirical geometric measurement, considering the apex of the most intense slice and each extremity of the 2D peak. The As_{2D} was also calculated as shown in Eq. (3),

$$As_{2D} = \frac{\sqrt{(\Delta^2 t_{Rf}/{}^2\omega)^2 + (\Delta^1 t_{Rb}/{}^1\omega)^2}}{\sqrt{(\Delta^2 t_{Rb}/{}^2\omega)^2 + (\Delta^1 t_{Rf}/{}^1\omega)^2}} \tag{3}$$

Table 5
Operating conditions of the five columns sets for HT-2D-GC-NCD experiments.

Set	Configuration	First column	Second column	Oven temperature	Inlet pressure
A		DB1-HT[a] 10 m × 0.32 mm × 0.1 μm	BPX-50[b] 0.5 m × 0.1 mm × 0.1 μm	90–360 °C; 2 °C/min	110 kPa
B	Normal	DB5-HT[c] 30 m × 0.32 mm × 0.1 μm	BPX-50[b] 1.5 m × 0.1 mm × 0.1 μm	90–360 °C; 2 °C/min	220 kPa
C		DB5-HT[c] 30 m × 0.32 mm × 0.1 μm	IL-59[d] 0.5 m × 0.1 mm × 0.08 μm	90–330 °C; 2 °C/min	130 kPa
D	Reversed	BPX-50[b] 30 m × 0.25 mm × 0.1 μm	DB1-HT[a] 1.5 m × 0.1 mm × 0.1 μm	90–360 °C; 2 °C/min	220 kPa
E		BPX-50[b] 10 m × 0.25 mm × 0.1 μm	DB1-HT[a] 5.5 m × 0.1 mm × 0.1 μm	90–360 °C; 2 °C/min	376 kPa

[a] Polydimethylpolysiloxane, Agilent.
[b] (50% Phenyl)polysilphenylene-siloxane, SGE.
[c] (5% Phenyl)methyl polysiloxane, Agilent.
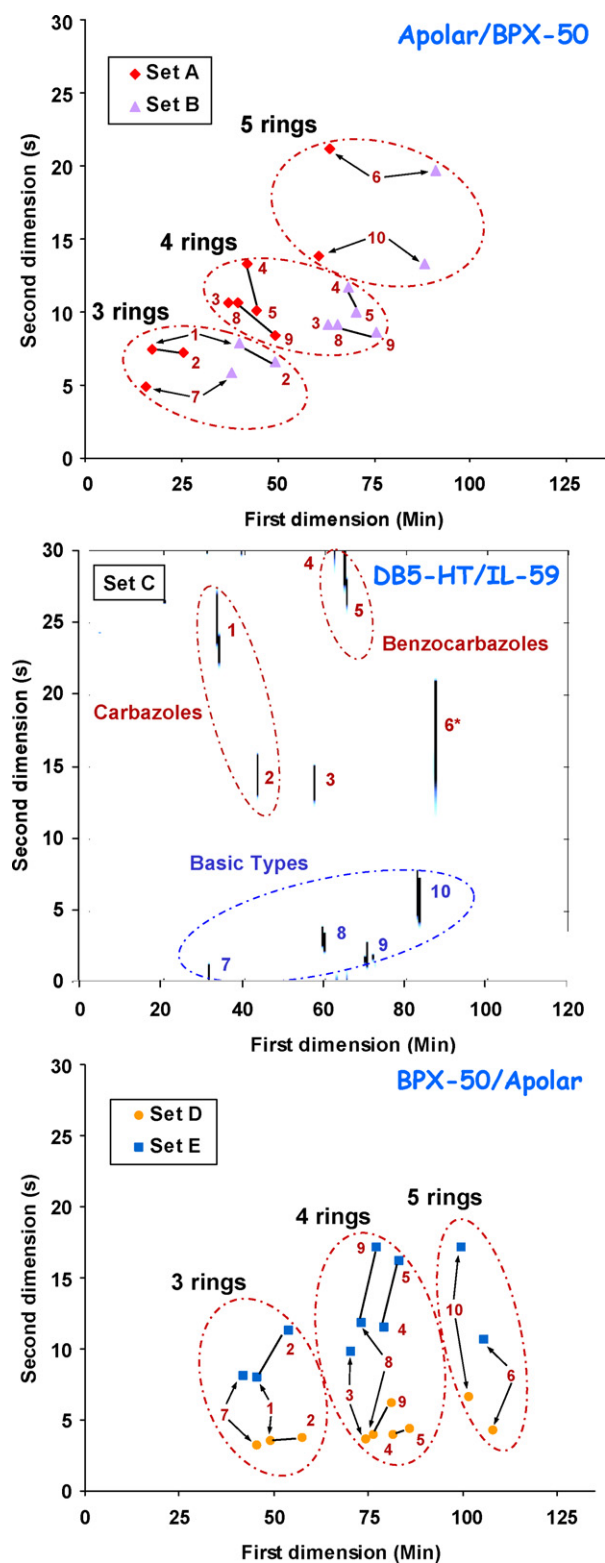[d] Dicationic ionic liquid, Supelco.

Fig. 1. 2D contour plots of the TM1 for the five implemented columns sets. For 2D contour plots of sets A, B and D, E, peak apices were compiled together. The labelling of model molecules follows the attributions in Table 1. See conditions in Table 5.

Fig. 2. Comparison of 2D resolutions by acido-basic properties (A), by alkylation (B) and by group type (C) for selected peaks in test mixture (TM1) contour plots of the five columns sets.

all peak retention time in each dimension. From 2D asymmetry evaluations, tailing 2D peaks were observed for all configurations (Fig. 3A).

In order to estimate the efficiency of a 2D system to separate a high number of solutes, the concept of 2D peak capacity production was applied [34], from Eq. (4),

$$\frac{n_{c,2D}}{^1T_R} = \frac{P_{\text{mod}}}{^1\omega} \times \frac{1}{^2\omega} \qquad (4)$$

where $n_{c,2D}$ is the peak capacity of the 2D system, ^1T_R is the first dimension running time, P_{mod} is the 2D modulation period, $^1\omega$ and $^2\omega$ are the first and the second dimension peak widths at 10%. The 2D peak capacity production (min^{-1}) was calculated from a few peaks of each set (Fig. 3B). Even if sets C and D show good results for acridine, set B provided overall best 2D peak capacity productions.

For the calculation of the peaks spreading on each 2D contour plot, the 2D space coverage [39–41] has been estimated (Fig. 3C). Although more developed methods could be used, a simple way was implemented in our case from Eq. (5),

$$\text{2D space coverage} = \frac{^1t_{Ra} - ^1t_{Rb}}{^1T_R} \times \frac{^2t_{Rc} - ^2t_{Rd}}{P_{\text{mod}}} \qquad (5)$$

where ^1T_R is the first dimension running time and P_{mod} is the 2D modulation period. The 2D occupied space was considered as a rectangle having for angles: the first ($^1t_{Rb}$) and the last ($^1t_{Ra}$) eluted peaks in the first dimension, and the corresponding ones in the second dimension ($^2t_{Rd}$) and ($^2t_{Rc}$). Among all of the columns con-

where $^1\omega$ and $^2\omega$ correspond to peak widths at 10%, respectively, in the first and in the second dimensions (for the most intense slice). Δt_{Rf} is the front difference between the apex and the lowest value of the overall peak retention time in each dimension. Δt_{Rb} is the back difference between the apex and the highest value of the over-
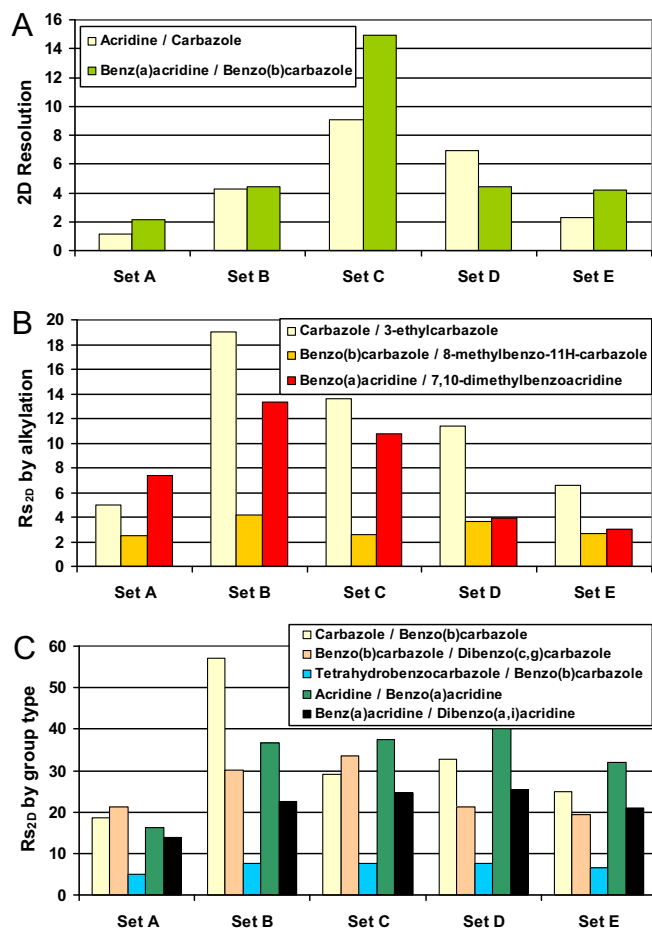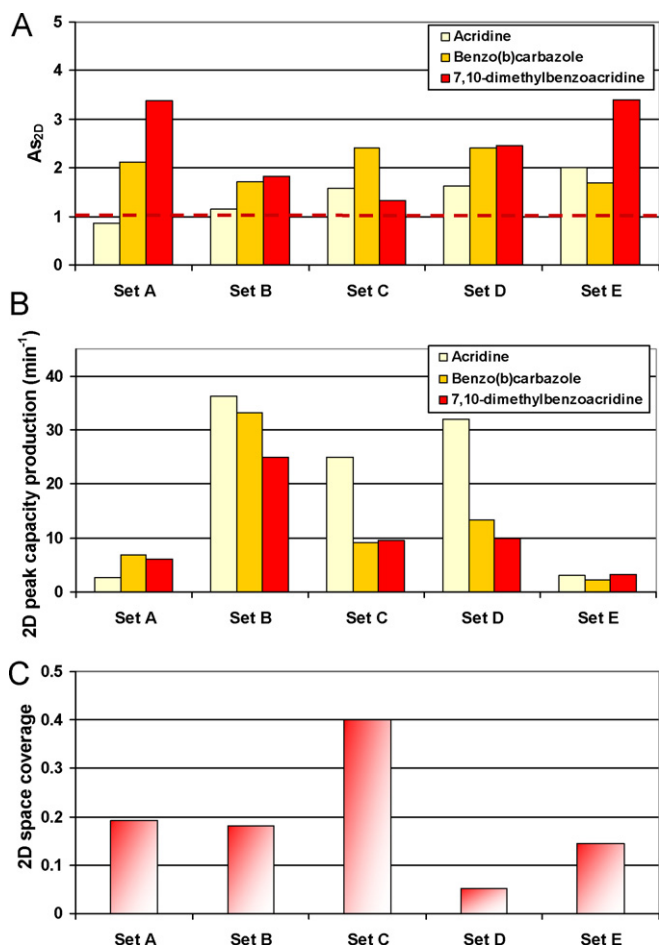
Fig. 3. Comparison of 2D asymmetries (A), 2D peak capacity productions (B) and 2D space coverages (C) for selected peaks in test mixture (TM1) contour plots of the five columns sets.

figurations, set C provided the best peaks spreading on the 2D contour plot, whereas set D gives results of less quality.

3.1.2. Choice of adapted 2D conditions

For an easier comparison of 2D columns sets, an overall quality index combining all of the 2D criteria was introduced. This approach allows the conversion into the same scale of values of the
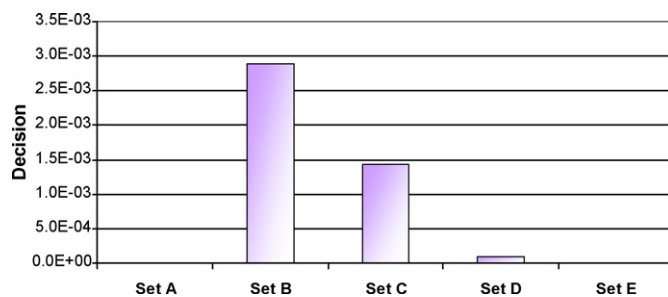

Fig. 4. Decision values for the five columns sets applied on the test mixture TM1.

different responses based on desired behaviours (desirability functions [42–44]). Briefly, the value corresponding to each individual 2D criterion was converted into a dimensionless number (or 'desirability value' (d_i)) within 0 and 1: 0 corresponds to a completely unacceptable value and 1 corresponds to a value totally fulfilling the requirements. Therefore, a desirability function was created for each 2D criterion taking into account the optimum conditions for each response. This was done considering linear functions for 2D resolutions, 2D peak capacity productions and 2D space coverages, and a polynomial function for 2D asymmetries. Then, an overall desirability (*Decision*) was calculated by combining all of the individual desirability values (or 'desirabilities') previously obtained, as shown in Eq. (6),

$$Decision = \left(\prod_{i=1}^{6} d_i \right)^{1/2} \tag{6}$$

where d_i are the desirability values. Thus, each desirability was taken into account without discrimination. Finally, sets B and C showed the best Decision values compared to the other columns sets (Fig. 4).

In order to confirm the results obtained by the investigations on the test mixture, sets B and C were implemented to analyse the same VGO (Fig. 5). As expected, for set B, compounds were scattered according to their aromatic rings number without any distinction based on their acido-basic type. Concerning set C, a clear distinction of 2D elution zones of the neutral N-compounds (i.e. carbazoles and benzocarbazoles) was observed. However, at high temperature the selectivity of IL-59 drastically decreases and column bleeding seems to occur (the recommended maximum temperature is 300 °C). Even if the ionic liquid phase showed important retentions for the "neutral" type compounds, it appears more adequate
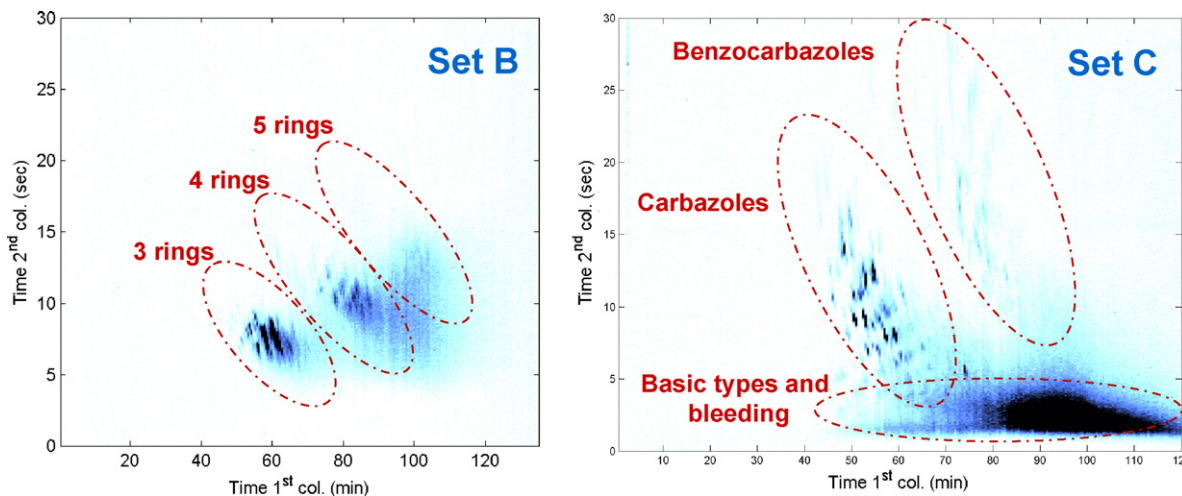
Fig. 5. 2D contour plots of the straight-run vacuum gas oil by sets B and C. See conditions in Table 5.

Straight-run VGO
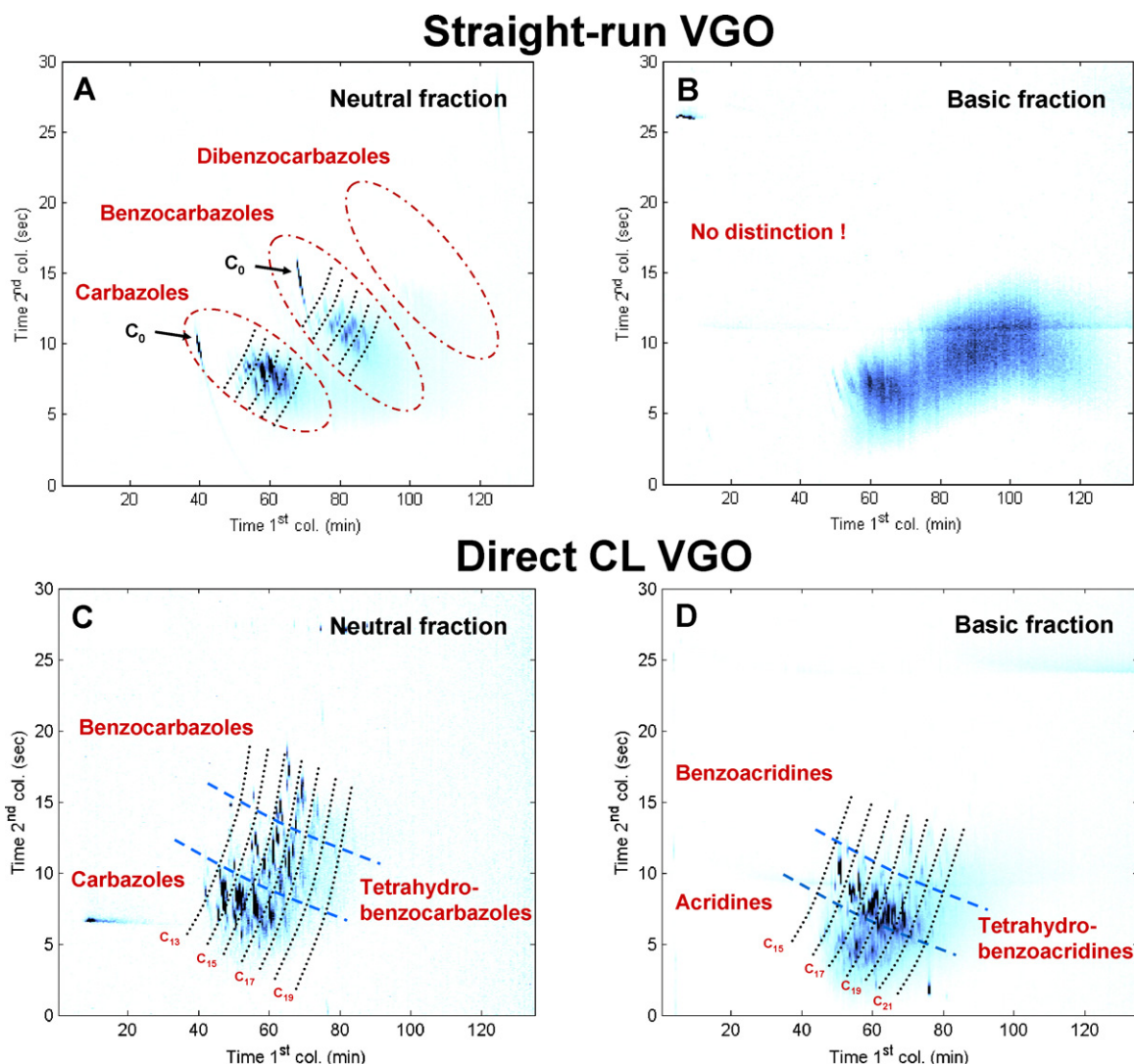
Direct CL VGO

Fig. 6. 2D contour plots of the straight-run VGO (neutral (A) and basic (B) fractions), and of the direct coal liquefaction (CL) VGO (neutral (C) and basic (D) fractions) by set B. See conditions in Table 5.

for lighter petroleum cuts such as middle distillates. Moreover, the basic N-compounds were not fully separated. Therefore, the choice of set B was confirmed for further investigations on real matrices.

3.2. Applications on two VGOs

A straight-run and a direct coal liquefaction (CL) vacuum gas oils were chosen for qualitative and quantitative characterizations of their nitrogen-containing compounds.

3.2.1. Integration of a pre-separation step

Although set B provided the best separation results, according to the Decision value, the distinction between acido-basic types was not straightforward. In order to access to it, a pre-separation step was performed prior to the 2D-GC experiments. After an overview of the literature, it appears that the solid/liquid fractionation, especially by ion-exchange resins [45], is the most efficient way to separate nitrogen-containing compounds in two fractions: basic and neutral types. Therefore a sulfonic acid resin type, Amberlyst A-15, was used. The fractionation into a neutral and a basic matrix was obtained thanks to the different affinities of N-compounds towards the resin, and to the use of ammonium based mixtures. The proportion of each nitrogen atom type was evaluated in each fraction

which allowed us to establish enrichment data (i.e. the separation selectivity) (Table 6). Thus, collected fractions for the two VGOs were deeply enriched by a majority of one acido-basic type, so that they can be considered as representative of their neutral or basic N-compounds.

3.2.2. Identification of 2D elution zones

Each basic and neutral fraction coming from both VGOs was analysed using set B (Fig. 6). The identification by retention times of model compounds was preferred over the hyphenation with a time-of-flight mass spectrometer, as mass spectra libraries are known to be limited for high molecular mass compounds. Therefore two extended test mixtures were implemented, the first containing basic N-compounds (TM2), and the second one containing neu-

Table 6
Results of separation selectivity of the ion-exchange chromatographic separation for both VGOs.

		% N_{basic}	% $N_{neutral}$
Conventional VGO	Neutral fraction	ε	≈ 100
	Basic fraction	86	14
Direct coal liquefaction VGO	Neutral fraction	3	97
	Basic fraction	≈ 100	ε
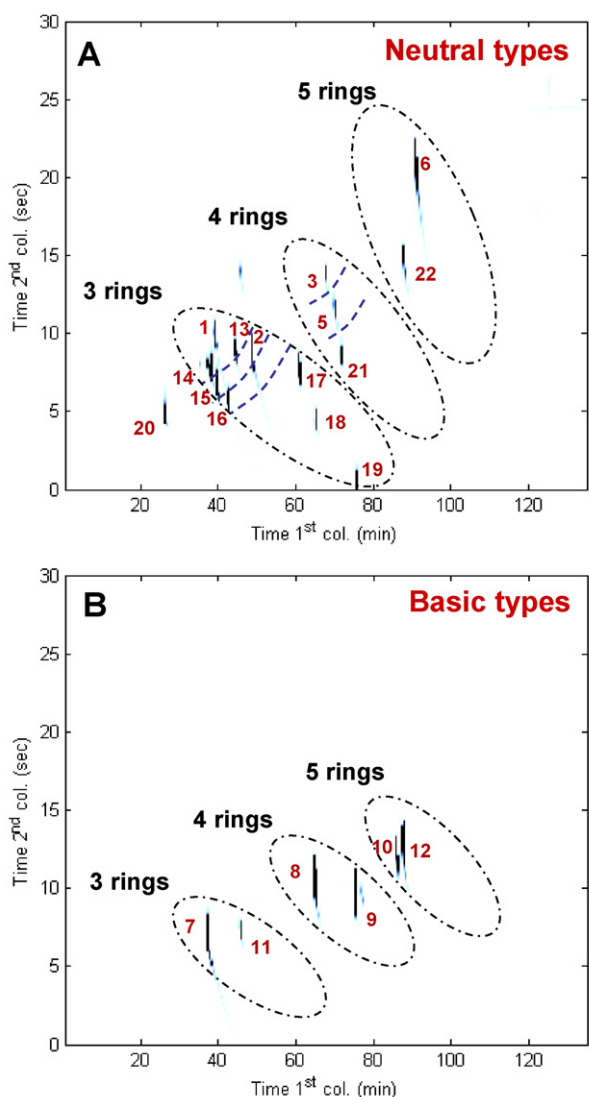
Fig. 7. 2D contour plots of test mixtures TM2 (B) and TM3 (A) by set B. The labelling of model molecules follows the attributions in Table 1. See conditions in Table 5.

tral N-compounds (TM3). Corresponding 2D contour plots by the analysis with set B are shown in Fig. 7. It is to be pointed out that N-compounds which are directly alkalized on their nitrogen atom, eluted with lower first and second dimension times on the 2D contour plot: for example compounds labelled 14, 15 and 16. This can be explained by a decrease of their polarity and boiling point due

to the disappearance of the strong hydrogen bonding. This distinction could be particularly interesting for the study of conversion processes, owing to their expected difference of reactivity.

Consequently, an extended identification was performed on each fraction of the two VGOs. Samples were spiked with reference N-compounds in order to adjust the offset of the relative retention times of second dimension. For instance, for the neutral fraction of the straight-run (Fig. 6A) VGO, the spiking was carried out using C_0-carbazole and C_0-benzocarbazole. Then, a detailed characterization was performed for this neutral fraction, whereas no distinction was achieved for the basic fraction of the straight-run VGO. This seems to be due to a too low content of basic N-compounds in this sample, as well as to a lack of selectivity towards these species.

Concerning the direct coal liquefaction VGO, an extended characterization of both fractions was achieved. Contrary to what was observed for the straight-run VGO, much more details were obtained for the basic fraction. This can be explained by the higher basic nitrogen content and the lower boiling point range of N-compounds, which both promote higher 2D resolutions. Moreover, intermediate 2D elution zones between the three N-aromatic classes (carbazoles and acridines) and the four N-aromatic classes (benzocarbazoles and benzoacridines) were observed in both fractions of this sample. Actually, this is consistent with the retention times of naphtheno N-aromatic model molecules: tetrahydrobenzocarbazoles and tetrahydrobenzoacridines. These observations are in agreement with the nature of these matrices and the involved process, which induces the formation of partially hydrogenated aromatic structures.

3.2.3. Quantification attempt

Analytical performances such as equimolarity and sensitivity of the NCD detector were checked before running each real sample. This was performed by using a GC-NCD analysis of a test mixture containing reference N-compounds with different molecular structures (aniline, carbazole and acridine) [15,20]. The quantification limit (less than 3 pg N/s) was checked according to DIN 32645. The equimolar response of the NCD detector was also evaluated by calculating the elementary response of nitrogen. Thereby, a bias less than 5% relative was found. The method was also found to be reproducible, based on repeated measurements ($n = 5$), the relative error within a 99% confidence remained below 5%. Concerning the 2D-GC analysis, N-compounds were quantified by normalization of the full area of the 2D contour plot to 100% of the basic or neutral nitrogen content.

Group type quantification results are in Table 7 for both VGOs. The proportion of each N-group type was determined for neutral and basic fraction. As each fraction was considered representative of the total amount of neutral or basic compounds, raw data were corrected using the original ratio between neutral and basic nitrogen content. Concerning the direct coal liquefaction VGO,
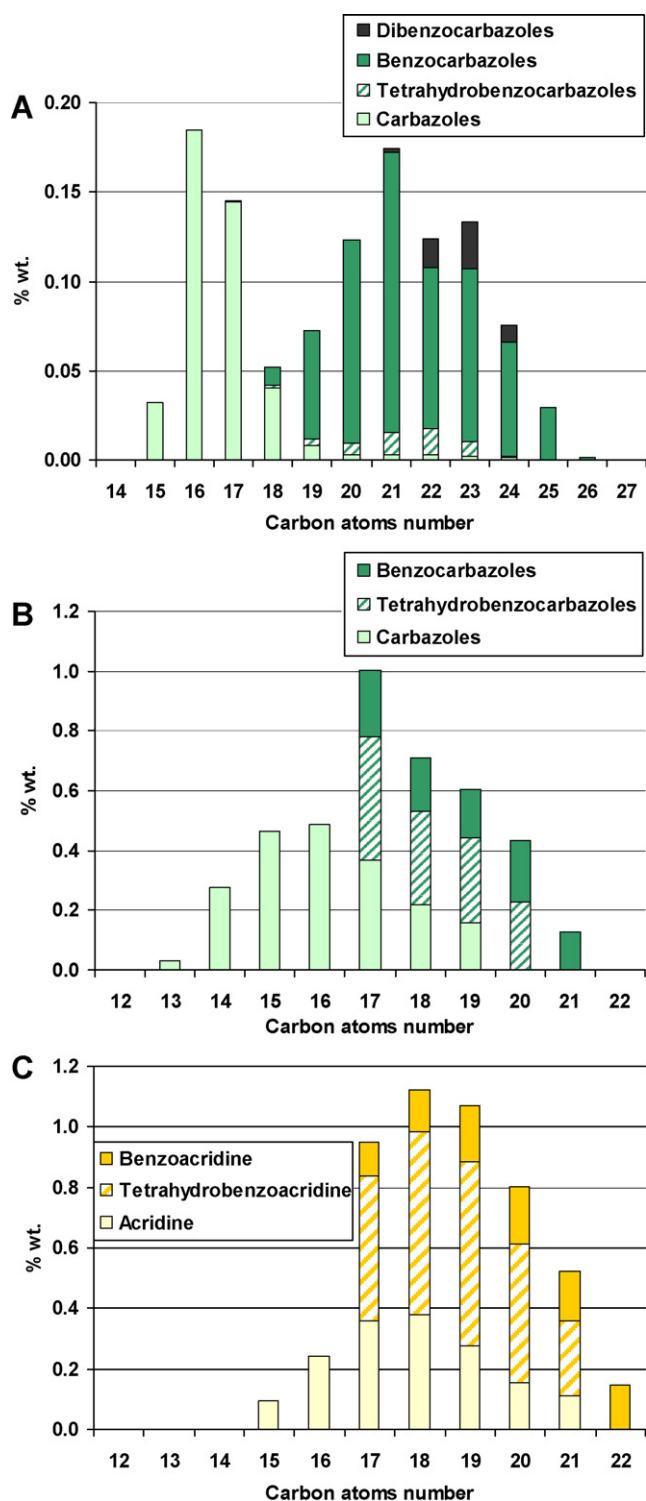
Table 7
Group type quantification of N-compounds in the two VGOs by HT-2D-GC-NCD combined with a previous ion-exchange chromatography.

Family	SR VGO			Direct LC VGO		
	In neutral fraction (% N)	In basic fraction (% N)	Total (ppm N)	In neutral fraction (% N)	In basic fraction (% N)	Total (ppm N)
Neutrals			601			2893
Carbazole	42.6		256.1	41.9		1212.8
Tetrahydrocarbazole	3.7		22.0	33.6		971.5
Benzocarbazole	49.6		298.4	20.8		600.5
Dibenzocarbazole	4.1		24.5	3.7		108.2
Basics			235			3255
Acridine		n.d.	–		28.6	930.8
Tetrahydroacridine		n.d.	–		51.2	1666.6
Benzoacridine		n.d.	–		16.3	531.5
Dibenzoacridine		n.d.	–		3.9	126.2

n.d.: not determined.

Fig. 8. Group type quantification by carbon atoms number for N-compounds of the straight-run VGO (A for neutrals) and the direct liquefaction VGO (B for neutrals and C for basics). HT-2D-GC conditions of set B combined with the pre-separation by acido-basic properties.

sents a breakthrough advance for the study of heavy petroleum samples, and they can be very interesting for process studies, in particular by kinetic modelling [46]. Even if high resolutions were obtained for the lightest N-compounds of VGO (i.e. from direct coal liquefaction, especially for basic compounds), the separation of the heaviest ones appears unattainable due to the low selectivity of stationary phases at high temperature. In order to obtain an extended identification, the application of these operating conditions with a mass spectrometer combined with an updated MS library could confirm more precisely the 2D elution zones, including those of isomeric homologues.

3.3. Conclusion

The hyphenation of HT-2D-GC with a specific NCD detector was implemented in this study. Several combinations of stationary phases were investigated (normal and reversed), especially the most thermal stable polar ones including an ionic liquid phase. Although this last one placed in second dimension allowed to enhance the separation between "neutral" and "basic" type N-compounds, its selectivity seems drastically decreased at high temperature. Finally a combination of an apolar column and a mid-polar one (BPX-50) was found to give the best results after the monitoring of 2D separation criteria. The application of these conditions (combined with an ion-exchange chromatography) to two vacuum gas oils, led to an innovative group type quantification by carbon atoms number. These results are a first attempt to obtain quantitative distributions of nitrogen-containing compounds in heavy matrices. However, at high temperature conditions, a limited selectivity was observed in particular towards heavy basic N-compounds. Finally results shown throughout this study can be directly integrated in hydroprocessing studies via molecular reconstruction schemes. This work also represents an insight into the understanding of the behaviour of high aromatic N-compounds by GC × GC.

References

[1] M.C. Loeffler, N.C. Li, Fuel 64 (1985) 1047.
[2] I. Merdrignac, D. Espinat, Oil Gas Sci. Technol. 62 (2007) 7.
[3] M. Sau, K. Basak, U. Manna, M. Santra, R.P. Verma, Catal. Today 109 (2005) 112.
[4] H.M. Chishti, P.T. Williams, Fuel 78 (1999) 1805.
[5] F. Jimenez, V. Kafarov, A. Nunez, Chem. Eng. J. 134 (2007) 200.
[6] E.C. Oliveira, M.C.V. de Campos, M.R.A. Rodrigues, V.F. Perez, M.I.S. Melecchi, M.G.R. Vale, C.A. Zini, E.B. Caramao, J. Chromatogr. A 1105 (2006) 186.
[7] J. Blomberg, P.J. Schoenmakers, U.A.T. Brinkman, J. Chromatogr. A 972 (2002) 137.
[8] J.C. Giddings, J. High Resolut. Chromatogr. 10 (1987) 319.
[9] H.J. Cortes, B. Winniford, J. Luong, M. Pursch, J. Sep. Sci. 32 (2009) 883.
[10] J. Beens, J. Blomberg, Compreh. Two Dimen. Gas Chem. 55 (2009) 149.
[11] F. Adam, D. Thiebaut, F. Bertoncini, M. Courtiade, M.C. Hennion, J. Chromatogr. A 1217 (2010) 1386.
[12] C. von Muehlen, E.C. de Oliveira, P.D. Morrison, C.A. Zini, E.B. Caramao, P.J. Marriott, J. Sep. Sci. 30 (2007) 3223.
[13] L.L.R. van Stee, J. Beens, R.J.J. Vreuls, U.A.T. Brinkman, J. Chromatogr. A 1019 (2003) 89.
[14] F.C.-Y. Wang, W.K. Robbins, M.A. Greaney, J. Sep. Sci. 27 (2004) 468.
[15] F. Adam, F. Bertoncini, N. Brodusch, E. Durand, D. Thiebaut, D. Espinat, M.C. Hennion, J. Chromatogr. A 1148 (2007) 55.
[16] F. Adam, F. Bertoncini, C. Dartiguelongue, K. Marchand, D. Thiebaut, M.C. Hennion, Fuel 88 (2009) 938.
[17] C. von Muhlen, E.C. de Oliveira, C.A. Zini, E.B. Caramao, P.J. Marriott, Energy Fuels 24 (2010) 3572.
[18] K.M. Van Geem, M.F. Reyniers, G.B. Marin, Oil Gas Sci. Technol. 63 (2008) 79.
[19] P. Wiwel, B. Hinnemann, A. Hidalgo-Vivas, P. Zeuthen, B.O. Petersen, J.O. Duus, Ind. Eng. Chem. Res. 49 (2010) 3184.
[20] N. Revellin, H. Dulot, C. Lopez-Garcia, F. Baco, J. Jose, Energy Fuels 19 (2005) 2438.
[21] I.P. Fisher, P. Fischer, Talanta 21 (1974) 867.
[22] A. Fafet, J. Bonnard, F. Prigent, Oil Gas Sci. Technol. 54 (1999) 453.
[23] C.A. Hughey, S.A. Galasso, J.E. Zumberge, Fuel 86 (2007) 758.
[24] T. Dutriez, M. Courtiade, D. Thiebaut, H. Dulot, F. Bertoncini, J. Vial, M.C. Hennion, J. Chromatogr. A 1216 (2009) 2905.

an extended quantification was performed since basic nitrogen-containing compounds are fully resolved in the 2D contour plot.

Data (by ppm N) obtained by the quantification of carbon atoms number and by group type, were converted into weight percentages *via* the contribution of the nitrogen atom in molecular weights. In Fig. 8, results are organized by neutral or basic type for each VGO. The deeper quantitative characterization of N-compounds repre-

[25] T. Dutriez, M. Courtiade, D. Thiebaut, H. Dulot, F. Bertoncini, M.C. Hennion, J. Sep. Sci. 33 (2010) 1787–1796.
[26] T. Dutriez, M. Courtiade, D. Thiebaut, H. Dulot, M.C. Hennion, Fuel 89 (2010) 2338.
[27] T. Dutriez, M. Courtiade, D. Thiebaut, H. Dulot, J. Borras, F. Bertoncini, M.C. Hennion, Fuel 89 (2010) 2338–2345.
[28] L. Fang, S. Kulkarni, K. Alhooshani, A. Malik, Anal. Chem. 79 (2007) 9441.
[29] D.W. Armstrong, T. Payagala, L.M. Sidisky, LC–GC Eur. 22 (2009) 459.
[30] J.L. Anderson, D.W. Armstrong, Anal. Chem. 77 (2005) 6453.
[31] T. Payagala, Y. Zhang, E. Wanigasekara, K. Huang, Z.S. Breitbach, P.S. Sharma, L.M. Sidisky, D.W. Armstrong, Anal. Chem. 81 (2008) 160.
[32] J.V. Seeley, S.K. Seeley, E.K. Libby, Z.S. Breitbach, D.W. Armstrong, Anal. Bioanal. Chem. 390 (2008) 323.
[33] V.R. Reid, J.A. Crank, D.W. Armstrong, R.E. Synovec, J. Sep. Sci. 31 (2008) 3429.
[34] W.C. Siegler, J.A. Crank, D.W. Armstrong, R.E. Synovec, J. Chromatogr. A 1217 (2010) 3144.
[35] E.C. Oliveira, M.C.V. de Campos, A.S. Lopes, M.G.R. Vale, E.B. Caramao, J. Chromatogr. A 1027 (2004) 171.
[36] J. Beens, M. Adahchour, R.J.J. Vreuls, K. van Altena, U.A.T. Brinkman, J. Chromatogr. A 919 (2001) 127.
[37] S. Peters, G. Vivo-Truyols, P.J. Marriott, P.J. Schoenmakers, J. Chromatogr. A 1146 (2007) 232.
[38] R.B. Gaines, G.S. Frysinger, J. Sep. Sci. 27 (2004) 380.
[39] D. Ryan, P. Morrison, P. Marriott, J. Chromatogr. A 1071 (2005) 47.
[40] B. Omais, M. Courtiade, N. Charon, A. Quignard, D. Thiebaut, J. Chromatogr. A, submitted for publication.
[41] C. Cordero, P. Rubiolo, B. Sgorbini, M. Galli, C. Bicchi, J. Chromatogr. A 1132 (2006) 268.
[42] D.L. Massart, B.G.M. Vandeginste, L.M.C. Buydens, Handbook of Chemometrics and Qualimetrics, Part A, Elsevier, Amsterdam, 1997.
[43] G. Derringer, R. Suich, J. Qual. Technol. 12 (1980) 214.
[44] J. Vial, M. Cohen, P. Sassiat, D. Thiebaut, Curr. Med. Res. Opin. 24 (2008) 2019.
[45] N. Revellin, Modélisation cinétique de l'hydrotraitement des distillats sous vide, Ph.D. thesis, Thèse de doctorat, Ecole Normale Supérieure de Lyon, Lyon, 2004.
[46] N. Charon-Revellin, H. Dulot, C. Lopez-Garcia, J. Jose, Oil Gas Sci. Technol., 2010, (in press).